



Title	Equilateral-Triangular Shape in 14C
Author(s)	Itagaki, N.; Otsuka, T.; Ikeda, K.; Okabe, S.
Citation	Physical Review Letters, 92(14), 142501 <a href="https://doi.org/10.1103/PhysRevLett.92.142501">https://doi.org/10.1103/PhysRevLett.92.142501</a>
Issue Date	2004-04-08
Doc URL	<a href="http://hdl.handle.net/2115/17209">http://hdl.handle.net/2115/17209</a>
Rights	Copyright © 2004 American Physical Society
Type	article
File Information	PRL92-142501.pdf



[Instructions for use](#)

## Equilateral-Triangular Shape in $^{14}\text{C}$

N. Itagaki,<sup>1,\*</sup> T. Otsuka,<sup>1,2,3</sup> K. Ikeda,<sup>2</sup> and S. Okabe<sup>4</sup>

<sup>1</sup>*Department of Physics, University of Tokyo, Hongo, Tokyo 113-0033, Japan*

<sup>2</sup>*The Institute of Physical and Chemical Research (RIKEN), Wako, Saitama 351-0198, Japan*

<sup>3</sup>*Center for Nuclear Study, University of Tokyo, Hongo, Tokyo 113-0033, Japan*

<sup>4</sup>*Center for Information and Multimedia Studies, Hokkaido University, Sapporo 060-0810, Japan*

(Received 3 September 2003; published 8 April 2004)

An equilateral-triangular shape of three  $\alpha$  clusters surrounded by excess neutrons is suggested for  $^{14}\text{C}$ , based on the molecular-orbit model. It is found that the attractive interaction between an excess neutron and an  $\alpha$  particle stabilizes the  $K^\pi = 0^+$  and  $3^-$  rotational bands, which demonstrates an equilateral-triangular symmetry. This  $K^\pi = 3^-$  band at 3 MeV below the  $^{10}\text{Be} + \alpha$  threshold energy corresponds to the experimentally observed band built on top of the second  $3^-$  state. A positive-parity rotational band ( $0^+, 2^+, 4^+$ ) arises similarly. These two bands suggest a molecular  $3\alpha$  structure stabilized by the excess neutrons and can be viewed as a realization of the  $\alpha$  crystallization in the dilute nuclear medium.

DOI: 10.1103/PhysRevLett.92.142501

PACS numbers: 21.30.Fe, 21.60.Cs, 21.60.Gx, 27.20.+n

Atomic nuclei have been known to have not only a spherical shape but also various deformed shapes, for instance, ellipsoidal shapes. However, it has been a long-standing dream of nuclear structure physicists to find an equilateral-triangular shape. While various cluster structures with different shapes have been considered in light exotic nuclei [1–5], the triangular shape still remains beyond the explored frontiers.

When the system has an equilateral-triangular configuration comprised of three  $\alpha$  clusters ( $3\alpha$ ), a rotational band structure with  $K^\pi = 3^-$  should appear, in addition to  $K^\pi = 0^+$ . In  $^{12}\text{C}$ , a  $3^-$  state has been observed at  $E_x = 9.6$  MeV [6]. This state may correspond to the band head of the above-mentioned  $K^\pi = 3^-$  rotational band [7]. However, this  $3^-$  state is already above the  $3\alpha$  threshold by about 2 MeV, suggesting that no bound system can be expected with a triangular configuration. Moreover, a large resonance width is expected for such  $4^-$  and  $5^-$  states, making their observation extremely difficult. Thus, it is unlikely that one can study the triangular shape by studying  $^{12}\text{C}$ . On the contrary, we demonstrate that in neutron-rich C isotopes this band becomes bound owing to the attraction produced by excess neutrons around the  $3\alpha$  core.

In this Letter, we start by introducing a microscopic model, in which the  $\alpha$ -cluster degree of freedom is exploited to predict quantitatively the level structure of the cluster band up to the 15-MeV region. The model space is  $\alpha + \alpha + \alpha + n + n$ . It seems crucial to incorporate the 5-body dynamics properly, while the  $\alpha$ -breaking effect is included at the level of the antisymmetrization. Since the neutrons around the three  $\alpha$  clusters are weakly bound, and may move over the whole region of the triangular configurations, we employ the molecular-orbital (MO) model, where wave functions of these neutrons can be spread as needed and yet the antisymmetrization with

constituents of the  $\alpha$  clusters is fulfilled. The MO method has been successfully applied to the structure of systems with two  $\alpha$  clusters and excess neutrons [5,8].

The total wave function of  $^{14}\text{C}$  is given by a superposition [i.e., generator coordinate method (GCM)] of basis states (with coefficients  $\{c_{ij}^K\}$ ). Each nucleon is represented by a Gaussian wave packet and is fully antisymmetrized with all others including those in  $\alpha$  clusters:

$$\Phi(^{14}\text{C}) = \sum_{K,i,j} c_{ij}^K P_{MK}^J \mathcal{A}\{(\phi_1^{(\alpha)} \phi_2^{(\alpha)} \phi_3^{(\alpha)})_i \times [(\psi_1^{(n)} \chi_1)(\psi_2^{(n)} \chi_2)]_j\}. \quad (1)$$

The sum is taken over the  $K$  quantum number, positions of  $\alpha$  clusters ( $i$ ), and configurations of the neutrons ( $j$ ). The amplitudes  $\{c_{ij}^K\}$  are determined by diagonalizing the Hamiltonian matrix after the projection of the angular momentum. Each of the three  $\alpha$  clusters ( $\phi_k^{(\alpha)}$ ,  $k = 1, 2, 3$ ) consists of two protons and two neutrons:

$$\phi_k^{(\alpha)} = G_{\vec{R}_{\alpha k}}^{p\uparrow} G_{\vec{R}_{\alpha k}}^{p\downarrow} G_{\vec{R}_{\alpha k}}^{n\uparrow} G_{\vec{R}_{\alpha k}}^{n\downarrow} \chi_{p\uparrow} \chi_{p\downarrow} \chi_{n\uparrow} \chi_{n\downarrow}, \quad (2)$$

$$G_{\vec{R}_{\alpha k}} = \left(\frac{2\nu}{\pi}\right)^{3/4} \exp[-\nu(\vec{r} - \vec{R}_{\alpha k})^2]. \quad (3)$$

Here, the central parameters of the three  $\alpha$  clusters ( $G_{\vec{R}_{\alpha 1}}$ ,  $G_{\vec{R}_{\alpha 2}}$ , and  $G_{\vec{R}_{\alpha 3}}$ ) describe the form of the triangular configuration, and  $\chi$  represents the spin-isospin eigenfunction. The oscillator parameter ( $\beta = 1/\sqrt{2\nu}$ ) is set equal to 1.46 fm. The wave function of each excess neutron [ $\psi_l^{(n)} \chi_l$ ,  $l = 1, 2$  in Eq. (1)] is expressed by a linear combination of local Gaussians  $\{G_{\vec{R}_m}\}$  with coefficients  $\{d_m^l\}$ ,

$$\psi_l^{(n)} \chi_l = \sum_m d_m^l G_{\vec{R}_m} \chi_l, \quad (4)$$

where  $G_{\vec{R}_m}$  represents a Gaussian wave function centered at  $\vec{R}_m$ .

The main aim of this Letter is to investigate a certain type of state as discussed below. The effective interaction is chosen so that one can describe reasonably well a system comprised of  $\alpha$  clusters with relative distances of a few fm and weakly bound neutrons. This means that the interaction must reproduce low-energy  $\alpha\text{-}\alpha$  and  $\alpha\text{-}n$  scattering but should be simple enough for treating the relevant many-body dynamics. Thus, we adopt the Volkov version No. 2 interaction [9] with the exchange parameters  $M = 0.6$  ( $W = 0.4$ ),  $B = H = 0.125$  for the central part, and the spin-orbit term of the so-called G3RS interaction [10] for the spin-orbit part as in [8]. All the parameters of this interaction were determined from the  $\alpha + n$  and  $\alpha + \alpha$  scattering phase shifts and the binding energy of the deuteron [11].

We first survey the intrinsic density distribution of an excess neutron, which gives us a basic picture. An equilateral-triangular configuration of three  $\alpha$ 's is assumed for simplicity. In Fig. 1, the intrinsic density distribution of one excess neutron before the angular momentum projection is presented by integrating along the  $z$  direction going through a given point on the  $xy$  plane. Note that the centers of three  $\alpha$ 's are on the  $xy$  plane. The distance between the centers of  $\alpha$  clusters is set to 3 fm, the most appropriate value for a clustering structure as seen below, while wave functions with various  $\vec{R}_m$  values in Eq. (4) are superposed. Figure 1 shows that, while the highest integrated density is at the center of gravity of the  $3\alpha$  triangle, the excess neutron is located also between two  $\alpha$ 's, and its density spreads farther outside the  $3\alpha$  triangle. Consequently, the neutron density distribution comes up with an inverse triangular shape, which can be contrasted with a possible naive expectation that the neutron density

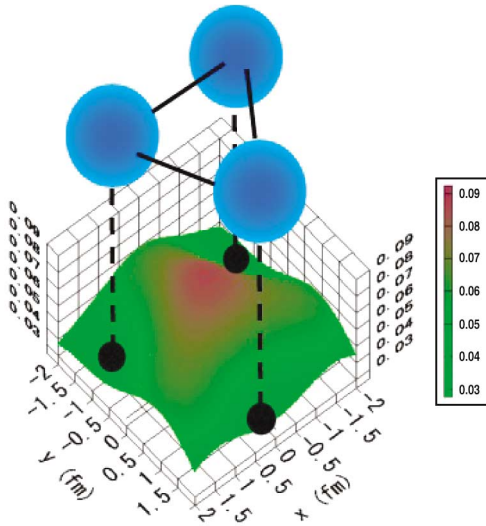


FIG. 1 (color). The density distribution of the excess neutron on the  $xy$  plane before the angular momentum projection. The spheres show the positions of the  $\alpha$  clusters. The distance between the centers of the  $\alpha$  clusters is set to 3 fm. The density is integrated over the  $z$  axis.

distribution has the same triangular shape as the three  $\alpha$  clusters.

Having the above basic picture, we evaluate energies more precisely, by implementing the angular momentum projection. Similar to the above calculation, we include about 200 wave functions with different values of  $\vec{R}_m$  before the projection for the two excess neutrons, keeping the  $\alpha\text{-}\alpha$  distance to 3 fm. Since the description of the two excess neutrons appears to be almost complete within the present model space with the fixed  $\alpha\text{-}\alpha$  distance, we call this calculation a “full neutron configuration.” After the  $J^\pi$  projection, the energies turn out to be  $-100.5$  and  $-91.0$  MeV for the  $0^+$  states and  $-91.6$  MeV for the  $3^-$  ( $K = 3$ ) state.

In order to clarify the mechanisms responsible for the stabilization of the triangular configuration, we introduce a model for the excess-neutron configurations. Therefore, next, we compare this full neutron configuration calculation with such model results.

In the model being considered, the lowest orbit for the excess neutron is the  $p$  wave in the  $z$  direction ( $p_z$ ), assuming that the three  $\alpha$ 's are on the  $xy$  plane. In this model, this wave function is approximated by a linear combination of two spherical Gaussians, whose centers are shifted in the  $z$  direction by  $b$  and  $-b$ :

$$\psi_z = G_{b\vec{e}_z} - G_{-b\vec{e}_z}. \quad (5)$$

This state yields a neutron density distribution concentrated near the center of the  $3\alpha$  and is especially relevant to the description of yrast states with relatively small  $\alpha\text{-}\alpha$  distances. Figure 2 exhibits the  $0^+$  and  $3^-$  ( $K = 3$ ) energies for this  $(p_z)^2$  configuration of excess neutrons. The equilateral-triangular shape is assumed for the three  $\alpha$ 's, while their distance is varied. Similar quantities are shown for comparison for  $^{12}\text{C}$ , where no excess neutrons are present.

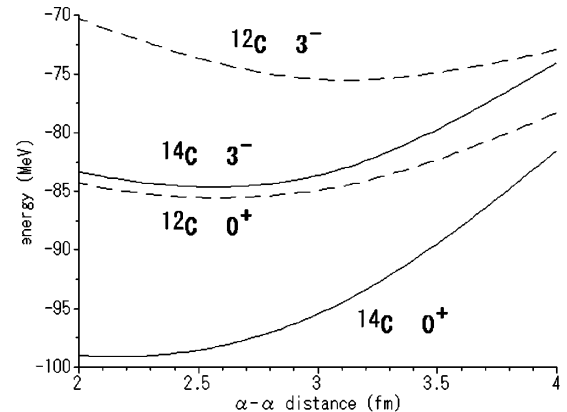


FIG. 2. The  $0^+$  and  $3^-$  ( $K = 3$ ) energies of  $^{12}\text{C}$  (dashed lines) and  $^{14}\text{C}$  (solid lines) as a function of the  $\alpha\text{-}\alpha$  distance. The equilateral triangular configuration of  $3\alpha$  is assumed. The solid lines represent  $^{14}\text{C}$  with the  $(p_z)^2$  configuration for the excess neutrons, and the dashed lines represent  $^{12}\text{C}$ .

Regarding the  $0^+$  states, the ground state of  $^{14}\text{C}$  has the energy minimum at a smaller distance ( $\sim 2$  fm) than in the  $^{12}\text{C}$  case. This suggests that the above  $(p_z)^2$  configuration for the neutrons is dominant in the ground state. After superposing the states with different distances, the energy of  $^{14}\text{C}$  becomes  $-99.8$  MeV, lower than that of  $^{12}\text{C}$  by about 13 MeV (experimental value is 13.1 MeV). For the  $3^-$  state, the equilateral-triangular shape of  $3\alpha$  is similarly stabilized in energy. The optimal  $\alpha$ - $\alpha$  distance of  $^{14}\text{C}$  ( $K = 3$ ) is about 2.5 fm ( $-84.6$  MeV), a little smaller than the value for  $^{12}\text{C}$ , and the energy is lower than that of  $^{12}\text{C}$  by about 10 MeV. However, this  $3^-$  energy is still much higher than the full neutron configuration result, and thus it is difficult to describe the  $3^-$  state by the  $(p_z)^2$  configuration alone. It is therefore necessary to include a neutron configuration of a different type.

As a second type of excess-neutron state, we now introduce the “bond” basis state  $\Phi(B)$ . We start with  $\alpha + ^{10}\text{Be}$  ( $\alpha + \alpha + 2n$ ) as a building block of  $^{14}\text{C}$ :

$$\Phi(B) = P_{MK}^J \mathcal{A}[\Phi(^{10}\text{Be}) \phi_3^{(\alpha)}], \quad (6)$$

$$\Phi(^{10}\text{Be}) = \phi_1^{(\alpha)} \phi_2^{(\alpha)} (\psi_1 \chi_1)(\psi_2 \chi_2). \quad (7)$$

In the subsystem  $^{10}\text{Be}$ , the two excess neutrons ( $\psi_1 \chi_1$  and  $\psi_2 \chi_2$ ) are rotating about the  $\alpha$ - $\alpha$  axis, where the spin-orbit interaction acts attractively [8]. Because of the antisymmetrization and angular momentum projection, in  $^{14}\text{C}$ , the pair of two excess neutrons between two  $\alpha$ 's is distributed equally among the three “molecular” bonds, and they are indistinguishable.

By superposing states with many  $\alpha$ - $\alpha$  distances and different triangular shapes, the energy levels of the negative parity states of  $^{14}\text{C}$  are calculated as presented in Fig. 3, where  $K$  mixing is performed. Not only  $(p_z)^2$ , but also the  $(p_z, 2s)$  and  $(2s)^2$  configurations for the excess neutrons, are included. Here, the  $2s$  orbit for the excess neutron is described as a linear combination of Gaussians, similar to the  $p$  orbits. Furthermore, more essentially for

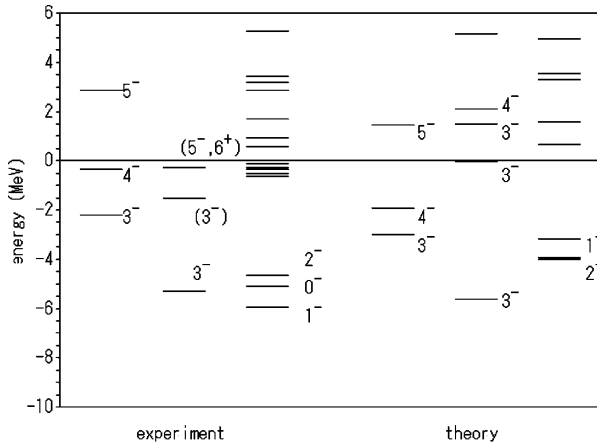


FIG. 3. The energy levels of  $^{14}\text{C}$  (negative parity states). The energy is measured from the  $^{10}\text{Be} + \alpha$  threshold energy.

$3^-$  states, the bond base  $[\Phi(B)]$  is also incorporated. Figure 3 shows results of these calculations in comparison with the experiment. The energy is measured from the  $^{10}\text{Be} + \alpha$  threshold (obtained to be  $-88.1$  MeV), which corresponds to  $E_x = 12.01$  MeV, experimentally. There are two  $3^-$  states below the threshold energy. The  $\alpha$ -cluster wave function of the first  $3^-$  state is dominated by components with smaller distances, and its nature is basically that of an octupole vibration on top of the shell-model-like ground state. On the other hand, the  $3_2^-$  state consists of cluster wave functions of larger distances ( $\sim 3$  fm) and appears to be a distinct example of a triangular cluster structure. Note that a large distance means a lower density. The energy levels of the  $3_2^-, 4_1^-,$  and  $5^-$  states display a rotational pattern as shown in the 4th column of Fig. 3. The levels put in the 5th column are calculated  $3^-, 4^-,$  and  $5^-$  states of another nature.

It is remarkable that experimental counterparts of these rotational states have been observed about 2 MeV below the  $^{10}\text{Be} + \alpha$  threshold, as shown in the 1st column. The situation is much different from  $^{12}\text{C}$ . In  $^{12}\text{C}$ ,  $3^-$  is already above the  $^8\text{Be} + \alpha$  threshold by 2 MeV and  $4^-$  and  $5^-$  have not been observed. In  $^{14}\text{C}$ , the candidate for the band head of this band corresponds to the observed second  $3^-$  state. It has been shown experimentally that members of this band are easily excited by  $\alpha$  transfer, which strongly suggests the  $\alpha$ -cluster structure of this band [12]. On the other hand, the first  $3^-$  state is well excited by a neutron-transfer reaction from the  $^{13}\text{C}$  nucleus, contrary to the second  $3^-$  state.

The energy levels of positive-parity states with respect to the  $^{10}\text{Be} + \alpha$  threshold energy are presented in Fig. 4. The calculated ground-state and second  $0^+$  energies are  $-103.1$  and  $-92.8$  MeV, respectively. The three states ( $0_2^+, 2_2^+,$  and  $4_2^+$ ) around the  $^{10}\text{Be} + \alpha$  threshold plotted in the 5th column have a band structure. In this energy region, the corresponding states have been observed experimentally, as shown in the 2nd column. The

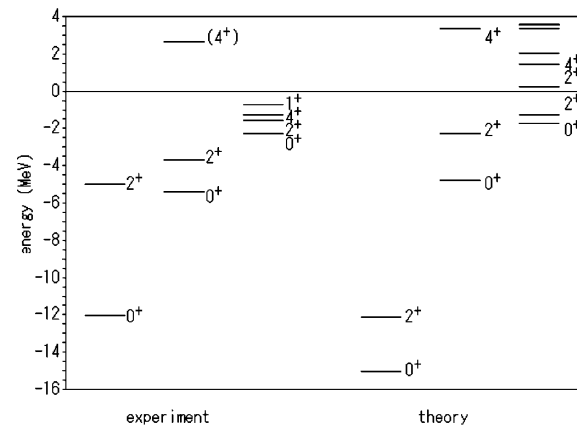


FIG. 4. The energy levels of  $^{14}\text{C}$  (positive parity states). The energy is measured from the  $^{10}\text{Be} + \alpha$  threshold energy.

calculated electromagnetic transition probabilities prove that these states are members of a rotational band. The  $B(E2 : 4_2^+ \rightarrow 2_2^+)$  (3.4 MeV) and the  $B(E2 : 2_2^+ \rightarrow 0_2^+)$  values are found to be 6.2 and 4.7 W.u., respectively, which are quite large for  $Z = 6$ .

In Fig. 4, the calculated first  $0^+$  and  $2^+$  levels are presented in the 4th column. The calculated energy spacing between them is too small (2.9 MeV), in comparison with the observed value of 7.01 MeV (1st column), which suggests other effects, for instance, the  $\alpha$ -breaking effect already discussed for  $^{12}\text{C}$  [13,14].

The appearance of the  $0^+$  and  $3^-$  rotational bands is one of the characteristic features of the triangular shape. In the case of the parity doublet seen in nuclei with octupole deformation, nearly degenerate  $0^+$  and  $1^-$  states appear [15]. Such a  $0^+-1^-$  doublet is seen also, if an  $\alpha$  cluster is weakly coupled, near the threshold energy like  $^{12}\text{C} + \alpha$  [16]. In the present case, however, the  $\alpha$ -clustering mechanism is different from the threshold case, and three  $\alpha$ 's are rather firmly fixed at the three top positions of the triangle. Excess neutrons are not localized to an  $\alpha$ , but move over the three  $\alpha$ 's. Thus, the situation is similar to a crystal. The kinetic energy of the relative motion of three  $\alpha$ 's is large, but the binding energy produced by the excess neutrons overcomes it. Because of this binding energy, the band heads come well below the threshold energy, in contrast to the threshold clustering. Thus, the clustering in exotic nuclei with excess neutrons can be characterized by the crystallization of clusters and by its stabilization due to the excess neutrons moving over those clusters like bond electrons. It has been known that the  $\alpha$  clustering emerges in dilute nuclear matter [17]. We stress that this low-density clusterization can be realized in bound states of a real nucleus owing to excess neutrons. We note the rms radii are large (about 2.6 fm) for the  $0_2^+$  and  $3^-$  states of  $^{14}\text{C}$ . Such a stable triangular configuration may be viewed in terms of the  $D_{3h}$  symmetry [18,19]. The electromagnetic transition probability of calculated rotational bands [ $B(E4 : 4_2^+ \rightarrow 0_2^+) = 177 e^2 \text{ fm}^8$ ,  $B(E3 : 3_2^- \rightarrow 0_2^+) = 28 e^2 \text{ fm}^6$ ] compares with those for the yrast band of  $^{12}\text{C}$  by an algebraic model [18,19] within about a factor of 2.

As we go farther away from the  $\beta$ -stability line, there are more excess neutrons. These excess neutrons yield additional binding energies, and one can expect bound clustering states in such heavier exotic nuclei. For instance, in the present approach, the cluster rotational band arises in  $^{16}\text{C}$  as bound states. Experimental and theoretical studies along this line will be intriguing.

In summary, in  $^{14}\text{C}$ , a  $K^\pi = 3^-$  rotational band structure, which reflects the equilateral-triangular shape of the

$3\alpha$ , appears well below the  $^{10}\text{Be} + \alpha$  threshold. The states correspond to an experimentally observed  $3^-$  state (9.80 MeV) and a  $4^-$  state (11.67). A positive-parity band ( $0^+$ ,  $2^+$ , and  $4^+$ ) of a similar nature also appears well below this threshold energy. The results suggest a new mechanism for the appearance of the bound cluster states in neutron-rich exotic nuclei with a rather dilute density distribution, having  $\alpha$  clusters at almost fixed relative positions and excess neutrons moving over them as well as near the triangle center.

We thank Professor W. von Oertzen, Professor H.G. Bohlen, Professor H. Horiuchi, Professor P. Ring, and Professor A. Gelberg for fruitful discussions. This work is supported in part by Grant-in-Aid for Specially Promoted Research (13002001) and by that for Scientific Research (13740145) from MEXT.

\*Electronic address: itagaki@phys.s.u-tokyo.ac.jp

- [1] M. Freer *et al.*, Phys. Rev. Lett. **82**, 1383 (1999).
- [2] W. von Oertzen, Z. Phys. A **354**, 37 (1996); **357**, 355 (1997).
- [3] Y. Kanada-En'yo, H. Horiuchi, and A. Doté, Phys. Rev. C **60**, 064304 (1999).
- [4] N. Itagaki, S. Okabe, K. Ikeda, and I. Tanihata, Phys. Rev. C **64**, 014301 (2001).
- [5] N. Itagaki, S. Hirose, T. Otsuka, S. Okabe, and K. Ikeda, Phys. Rev. C **65**, 044302 (2002).
- [6] F. Ajzenberg-Selove, Nucl. Phys. **A506**, 1 (1990).
- [7] Y. Fujiwara, H. Horiuchi, K. Ikeda, M. Kamimura, K. Katō, Y. Suzuki, and E. Uegaki, Prog. Theor. Phys. Suppl. **68**, 60 (1980).
- [8] N. Itagaki and S. Okabe, Phys. Rev. C **61**, 044306 (2000); **64**, 014301 (2001).
- [9] A. B. Volkov, Nucl. Phys. **74**, 33 (1965).
- [10] N. Yamaguchi, T. Kasahara, S. Nagata, and Y. Akaishi, Prog. Theor. Phys. **62**, 1018 (1979).
- [11] S. Okabe and Y. Abe, Prog. Theor. Phys. **61**, 1049 (1979).
- [12] W. von Oertzen, in *Proceedings of the International Conference on Nuclear Clusters: From Light Exotic to Superheavy Nuclei*, edited by R. Jolos and W. Scheid (EP Systema, Debrecen, 2003), p 31.
- [13] Y. Kanada-En'yo, Phys. Rev. Lett. **81**, 5291 (1998).
- [14] N. Itagaki, K. Hagino, T. Otsuka, S. Okabe, and K. Ikeda, Nucl. Phys. **A719**, 205c (2003).
- [15] P. A. Butler and W. Nazarewicz, Rev. Mod. Phys. **68**, 349 (1996).
- [16] H. Horiuchi and K. Ikeda, Prog. Theor. Phys. **40**, 277 (1968).
- [17] D. M. Brink and J. J. Castro, Nucl. Phys. **A216**, 109 (1973).
- [18] R. Bijker and F. Iachello, Phys. Rev. C **61**, 067305 (2000).
- [19] R. Bijker and F. Iachello, Ann. Phys. (N.Y.) **298**, 334 (2002).